

Significance of Hemodynamic Effects on the Generation of Atherosclerosis

Sang-Ho Suh*, **Hyung-Woon Roh**, **Dong-Joo Kim**

Department of Mechanical Engineering, Soongsil University, Seoul, Korea

Hyuck-Moon Kwon

Department of Internal Medicine, College of Medicine, Yonsei University, Seoul, Korea

Byoung-Kwon Lee

Department of Internal Medicine, College of Medicine, Inje University, Seoul, Korea

Atherosclerosis, which is a degenerative vascular disease, is believed to occur in the blood vessels due to deposition of cholesterol or low density lipoprotein (LDL). Atherosclerotic lumen narrowing causes reduction of blood flow due to hemodynamic features. Several hypothetical theories related to the hemodynamic effects have been reported: high shear stress theory, low shear stress theory, high shear stress gradient theory, flow separation and turbulence theory, and high pressure theory. However, no one theory clearly explains the causes of atherosclerosis. The objective of the present study was to investigate the mechanism of the generation of atherosclerosis. In the study, the database of Korean carotid and coronary arteries for geometrical and hemodynamic clinical data was established. The atherosclerotic sites were predicted by the computer simulations. The results of the computer simulation were compared with the *in vivo* experimental results, and then the pathogenesis of atherosclerosis by using the clinical data and several hypothetical theories were investigated. From the investigation, it was concluded carefully that the mechanism of the generation of atherosclerosis was related to the hemodynamic effects such as flow separation and oscillatory wall shear stress on the vessel walls.

Key Words : Atherosclerosis, Hemodynamic Hypotheses, Comparative Study, Hemodynamic Characteristics, Vision Technique, Computer Simulation

Nomenclature

Alphabetic letters

- A Coefficient of the diagonal term of the matrix
C Convective contributions from the six surrounding control volumes
SP Source term enhancing the diagonal dominance of the matrix
p Pressure [Pa]
q Index of Carreau model
u Velocity [m/s]

x Coordinate [m]

Greek symbols

- ϕ Dependant variables
 γ Shear rate [1/s]
 η_{∞} Apparent viscosity at infinite-shear-rate [Pa·s]
 η_0 Apparent viscosity at zero-shear-rate [Pa·s]
 λ Characteristic time [s]
 ρ Density [kg/m³]

* Corresponding Author,

E-mail rohlee@yahoo.com

TEL +82-2-824-0658, FAX +82-2-820-0668

Department of Mechanical Engineering, Soongsil University, Seoul, Korea (Manuscript Received September 23, 2004, Revised December 7, 2005)

Superscripts

i, j Tensor index

nb: Contributions of the neighbouring control volumes

p Control volume whose variables

1. Introduction

Atherosclerosis is associated with lipid deposition in the sub-endothelial space, intimal thickening, in smooth muscle cell proliferation, and plaque formation. Atherosclerosis, which is known as a degenerative disease, is believed to occur in the vascular system due to deposition of cholesterol and low-density lipoprotein (LDL) or thrombosis in blood vessels. Atherosclerosis narrows the arterial lumen, that is, the stenosis phenomenon in the blood vessel reduces the blood flow rate. Atherosclerotic plaques appear predominantly in the regions of the arterial bifurcations, the curved arterial segments and in the proximal lips of branches such as the abdominal aorta, carotid and coronary arteries. In particular, it has been speculated that atherosclerosis in the arteries occurred mainly due to hemodynamic effects. Atherosclerotic plaques reduce the capacity of circulating blood flow and increase blood pressure resulting in excessive pulsation and/or heart failure.

Advances in medical science and technology have kept pace with the civilization of human history and made great contributions to understand the etiology and pathogenesis of arterial diseases. Scientific approaches such as bioengineering and hemodynamics are important not only to give proper remedies and prescriptions to patients but also to trace the origin of diseases and to develop artificial organs and medical devices. In recent years physicians and researchers have shown increased interests in the role of hemodynamics and blood viscosity to the pathogenesis of arterial diseases (Texon et al., 1965, Fox et al., 1966, Tucker and Myron, 2001, Fry, 1972, Caro et al., 1971). Clinical studies have confirmed the results of hemodynamic studies in assessing atherosclerosis-related diseases. Results of hemodynamic studies include flow velocity, shear stress, flow separation and rheological properties of blood. The inter-relationship between diseases and blood flow characteristics in the arteries should be thoroughly understood. But in spite of massive research efforts and numerous

hypothesis, the initiating event in atherosclerosis has not been identified.

The objective of the present study was to investigate the mechanism of the generation of atherosclerosis. We have investigated the role of hemodynamics in the formation and development of atherosclerotic lesions. The hypotheses related to the hemodynamic effects will be tested by using computer simulation, in vitro and in vivo experimental studies. This study also aimed to develop software, which could generate three-dimensional vascular models automatically by the angiogram images and visualize the blood flows using the computer vision techniques.

2. Blood Vessel Models

To understand the generation of atherosclerosis, in-depth knowledge of blood flows through different human arteries is required. The basic vessel models were adopted based on the in vivo measurements using the angiography. It was found that the carotid and coronary arteries were favored sites for the formation of atherosclerosis (Fig. 1).

We have tried to establish the database of the carotid and coronary arteries for Korean subjects. Duplex scan (ATL Inc.) was used to obtain the images of the flow characteristics. And the geometric dimensions of the models were taken from the measured data by the angiography (Fig. 1(a) and (b)) (Lee et al., 2001, Suh et al., 2003).

For the computer simulation, the following methods and devices were used for the measurements of flow-velocity and pressure: the in-vivo hemodynamic data with the Doppler ultrasound by using a 3.5 MHz transducer (Cardiometrics, California, USA) and pressure wire with a 0.014 inch guide wire-mounted pressure sensor (Radi Medical Systems AB, Uppsala, Sweden). The measured velocity waveforms of the carotid and coronary arteries were presented in Fig. 2.

The reconstructed blood vessel models were obtained from 2 dimensional CT (Computed Tomography) images by using the vision techniques. The method consists of three distinguishable phases. The first phase performs a seg-

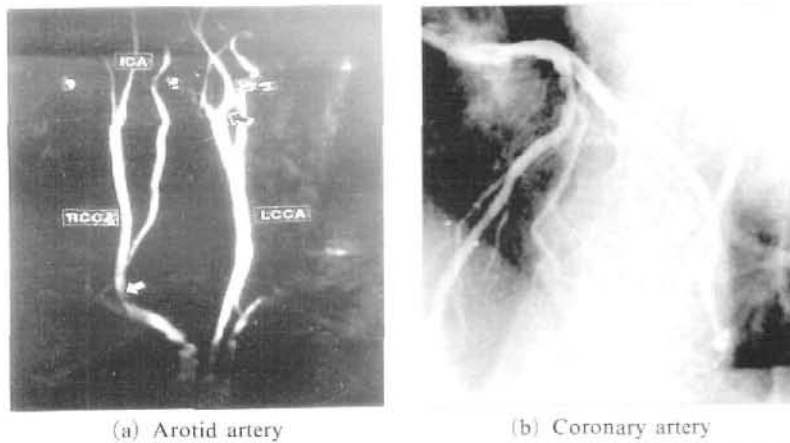
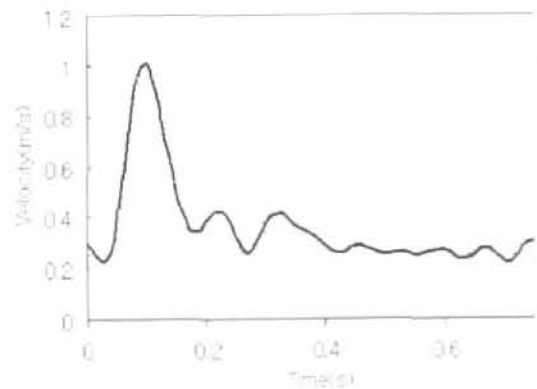
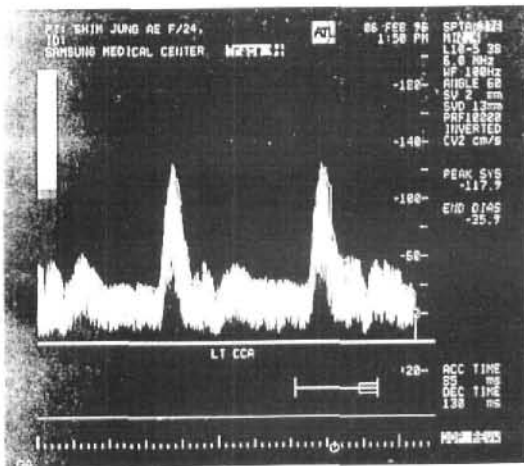
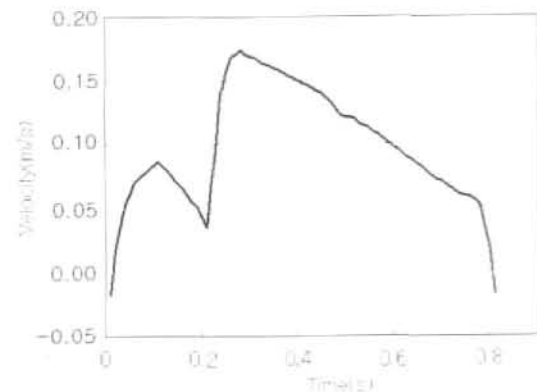
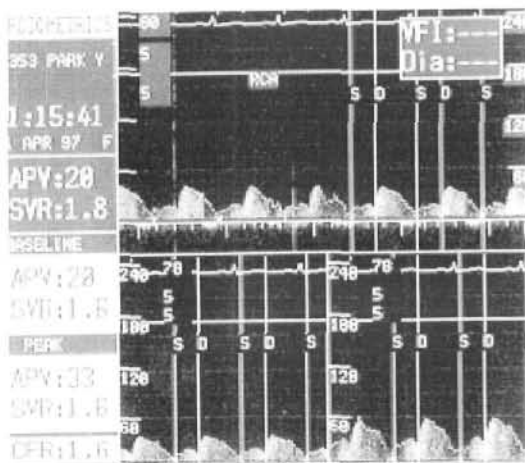


Fig. 1 Angiograms of the carotid and coronary arteries with atherosclerotic lesions



(a) Duplex scan signal and physiological waveform in the carotid artery



(b) Doppler ultrasound signal and physiological waveform in the coronary artery

Fig. 2 Physiological waveforms obtained by the in vivo experiments

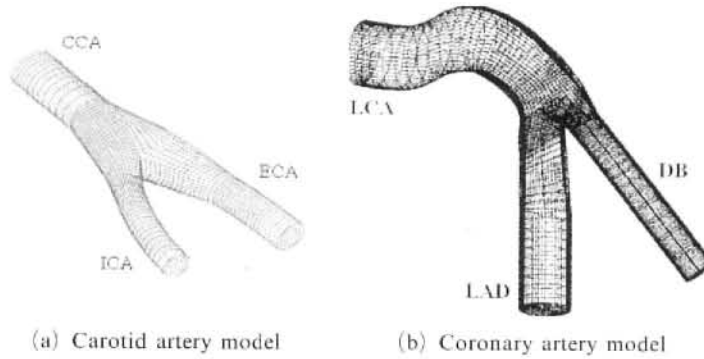


Fig. 3 Reconstructed blood vessel models using the developed vision technique

mentation of blood vessel area from the 2-dimensional CT images; the second phase extracts the contour of the blood vessel from the segmented blood vessel area; and the last phase generates a 3-dimensional blood vessel model from a multi-layer 2-dimensional CT images. To extract the blood vessel area from 2-dimensional CT images the segmentation algorithm was employed. After performing segmentation on the blood vessel area, the actual blood vessel areas could be extracted. In essence, the contour extraction on the blood vessel area was required to generate the 3-dimensional models of the blood vessel as like Fig. 3.

3. Computer Simulations

The following continuity and momentum equations were used for the computer simulation. (Suh et al, 1996; Cho et al., 2002)

$$\frac{\partial u_j}{\partial x_j} = 0 \quad (1)$$

$$\rho \left(\frac{\partial u_i}{\partial t} + u_j \frac{\partial u_i}{\partial x_j} \right) = - \frac{\partial p}{\partial x_i} + \eta \frac{\partial}{\partial x_j} \left(\frac{\partial u_i}{\partial x_j} + \frac{\partial u_j}{\partial x_i} \right) \quad (2)$$

where ρ , u_i , p , and η are density, velocity vector, pressure, and apparent viscosity, respectively. To take into account the rheological characteristics of blood, a constitutive equation that represents the apparent viscosity of blood as a function of shear rate is required. The Carreau model of Eq.

(3) was used to specify the apparent viscosity of blood.

$$\eta = \eta_\infty + (\eta_0 - \eta_\infty) [1 + (\lambda \dot{\gamma})^2]^{\frac{(q-1)}{2}} \quad (3)$$

where $\dot{\gamma}$ denotes the shear rate. η_∞ and η_0 are the apparent viscosity at infinite-shear-rate and zero-shear-rate, respectively. λ and q represent the characteristic time and index of this model, respectively. As the local shear rate in the flow field is calculated, the apparent viscosity of a non-Newtonian fluid could be determined by Eq. (3).

To analyse the blood flow problems effectively, we used the finite volume method. The continuity and momentum equations were used as the governing equations for the computer simulation. All equations have the same general conservative form

$$\frac{\partial(\rho\phi)}{\partial t} + \nabla \cdot (\rho\vec{v}\phi) - \nabla \cdot (\Gamma\nabla\phi) = S \quad (4)$$

The equation was integrated over each individual control volume to form the integral form of the equation which relates the behaviour of the variable ϕ at the center of the control volume to its neighbouring control volumes:

$$\int \frac{\partial(\rho\phi)}{\partial t} dV + \int \rho\phi\vec{v} \cdot \hat{n} dA - \int \Gamma\nabla\phi \cdot \hat{n} dA = \int S dV \quad (5)$$

The advection terms were discretized using the different discretized scheme to enhance stability.

With the convective terms in the momentum equations, particular problems arise in determining the convection coefficients from the node-centered velocity when it is actually required on the node faces. To overcome this problem, a special scheme was implemented in the code to deal with the mass source residuals and the velocity-pressure coupling. The velocity-pressure coupling was handled using different algorithm. The set of equations for a steady-state and an individual time step could be presented in matrix form as

$$A_p \phi_p - \sum_{nb} A_{nb} \phi_{nb} = SU \quad (6)$$

where subscript nb represents the contributions of the neighbouring control volumes and subscript p is the control volume whose variables are being solved. A_p is the coefficient of the diagonal term of the matrix and is given as

$$A_p = \sum_{nb} A_{nb} - SP + C_U - C_D + C_N - C_S + C_E - C_W + \frac{\rho V}{\Delta t} \quad (7)$$

where SP represents the source term enhancing the diagonal dominance of the matrix, the C -terms the convective contributions from the six surrounding control volumes, and the final term the storage term attributable to transient effects. The complete matrix is then solved using Stone's method. The fully implicit scheme was used to solve the physiological flow problem.

4. Mechanism of the Generation of Atherosclerosis

4.1 Review of the pressure-related hypothesis

The computer simulation was applied to investigate the relationship between arteriosclerosis and the pressure-related hypothesis. Atherosclerosis is often defined as a type of arteriosclerosis. Texon et al. (1965) asserted that low-pressure regions were the favored sites for the formations of atherosclerosis based on the Bernoulli's theory. And they reported that the endothelial cells at the surface of endothelium were separated to the SMC (Smooth Muscle Cell) by the applied suction action and the successive endothelial cells and SMC's were injured by the relating wall shear stress.

In Fig. 4 the pressure distributions, which were obtained by the computer simulation, were presented at the acceleration and deceleration phases. The blood flows in the artery were affected by the pressure differences according to the heart actions. The pressure distribution at the inlet region was higher than that at the outlet region. The pressure values were varied in the artery due to the geometric arrangements of the arterial system with respect to the curved area and bifurcated region. Atherosclerotic plaques are frequently observed at the bifurcation areas but not in straight sections before and after the bifurcations.

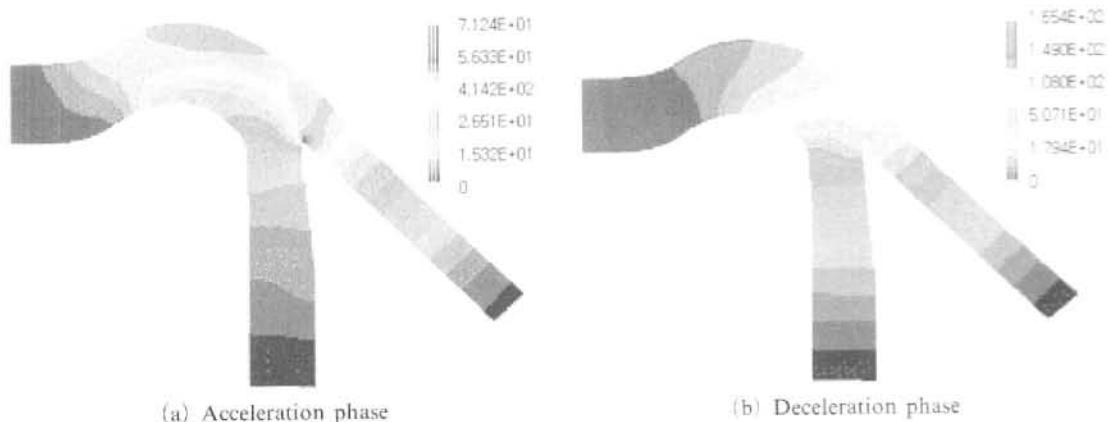


Fig. 4 Pressure contours of the physiologic blood flow in the left coronary artery model

The signification of the curved area is that atherosclerotic lesions frequently occurred along the inner wall of the curved segment. From the clinical data, arteriosclerosis occurred at very specific sites in the arterial system. As shown in Fig. 4 the results of the pressure distributions in the region of curved and bifurcated arterial segments showed a similar distribution when compared with the adjacent areas of the curved and bifurcated regions. No negative values of the transmural pressure appeared in the regions of the vessel walls. From the above results we found it very difficult to predict the cause of atherosclerosis by the pressure related hypothesis.

4.2 Review of Flow separation related hypothesis

In this section, the computer simulations and in vivo experiments were conducted to evaluate the relation between the origin of atherosclerosis and the flow separation related hypothesis. The velocity vectors during the acceleration and deceleration phases in the left coronary artery are presented in Fig. 5.

In considering the pulsatile waveform of phasic coronary blood flow, the velocity profiles of the acceleration and deceleration phases were represented. In the acceleration phase, there was no flow reversal on the curved area of the left

coronary artery.

Flow velocities along the inner wall were higher than those along the outer wall in the curved area of the left coronary artery. In serial cross-sectional velocity analysis, abrupt changes of the flow velocity and flow reversal showed mainly in the outer curved region of the left coronary artery above the bifurcation area. However, this flow reversal and formation of a recirculation area disappeared as the flow reached the bifurcation region, where the entrance flow was skewed toward the inner walls of the LAD (Left Anterior Descending) artery and the diagonal branch.

Because the blood flows varied significantly during a cardiac cycle, it was difficult to define the sites where atherosclerosis occurred using the streamlines at the acceleration and deceleration phases. The negative implication of eddy currents is the increased resistance to blood flow due to a tremendous increase in the friction of flow. This friction translates into fatigue injury to the endothelium.

The numerical results were presented for the flow velocities in the carotid artery bifurcation. The velocity profiles during the peak velocity ($t=0.1s$) and deceleration phase ($t=0.24s$) are presented in Fig. 6. The velocity profiles in the CCA (Common Carotid Artery) were parabolic

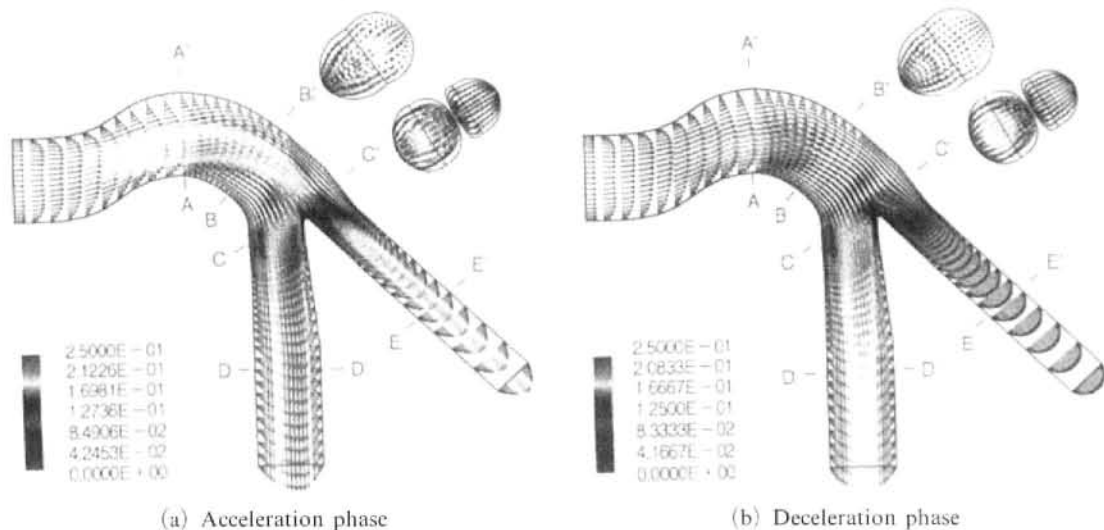


Fig. 5 Velocity vectors and secondary flows of the physiologic blood flow in the left coronary artery model

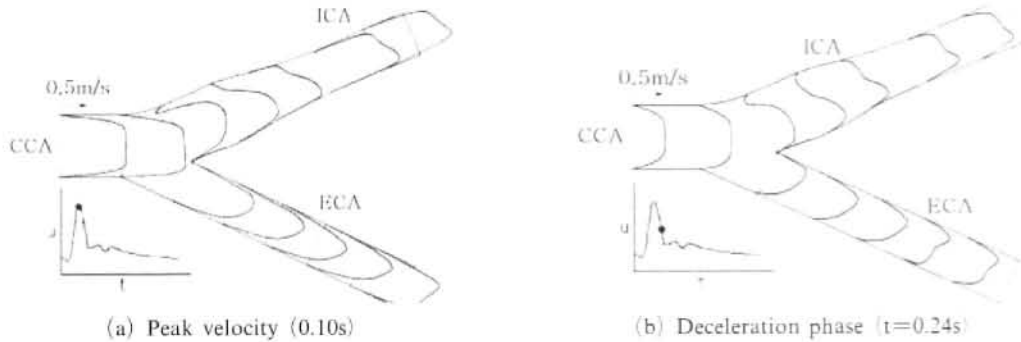


Fig. 6 Velocity profiles for the physiological flow

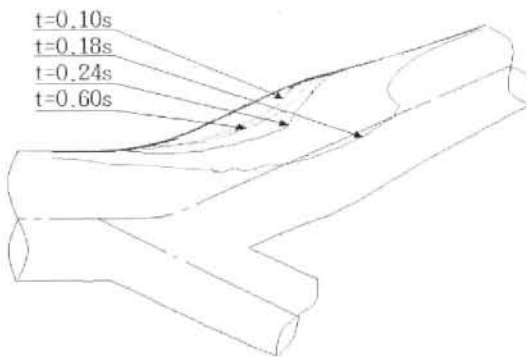


Fig. 7 Recirculation zone in the flow sinus of the ICA

in shape showing the symmetry with respect to the centerline. As the flow was bifurcated into the ICA (Internal Carotid Artery) and ECA (External Carotid Artery), the velocity profiles were skewed to the inner walls of both sides. The flows resumed their symmetry in the far downstream side. The recirculation zone was observed in the sinus of the ICA.

The flow in the ICA showed a relatively complex behaviour depending on place and time. Thus, recirculation zones with time variable were presented to illustrate the complex behaviours in the ICA as shown in Fig. 7. The lines in the figure were contour lines of zero axial velocity level. As the time increased in Fig. 7, the secondary flow regions expanded and shrank depending on the phasic time. The maximum recirculation zone occurred during the deceleration phase ($t=0.18s$). The reversed flow occupied about 51% of the sinus diameter in the branching plane. The secondary velocity vectors and the shaded con-

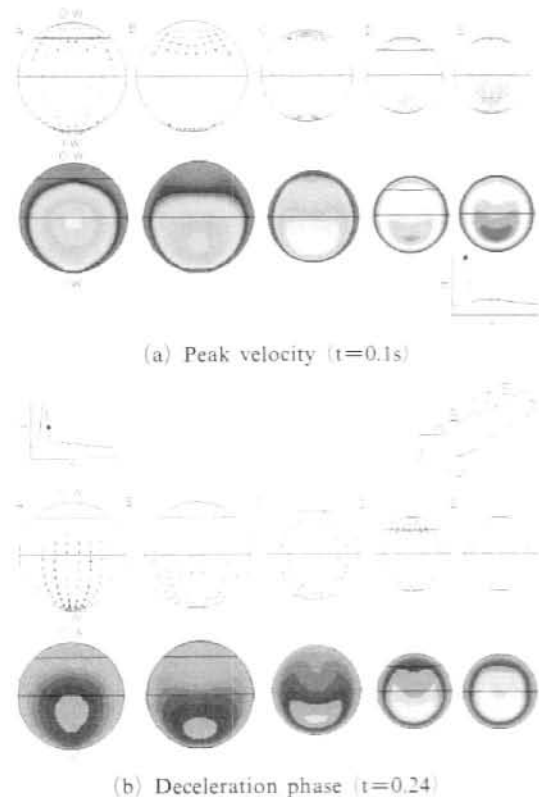


Fig. 8 Secondary velocity vectors and shade contours in the ICA

tours illustrated the flow recirculation at the specified flow cross-sections. The intensive secondary motion in the sinus was evident during the high flow rates. The secondary motion in Fig. 8 resulted from the superposition of the branching effect and the curvature effect. At the cross-section B (proximal of the sinus) the branching effect is dominant.

The recirculation zone was observed in the sinus of the ICA and the zone varied during the systole/diastole phase. The wall shear stress varied from the negative value to the positive value during a cycle. It was speculated that the abrupt change of the wall shear stress in the sinus might be responsible for the initial formation of atherosclerosis.

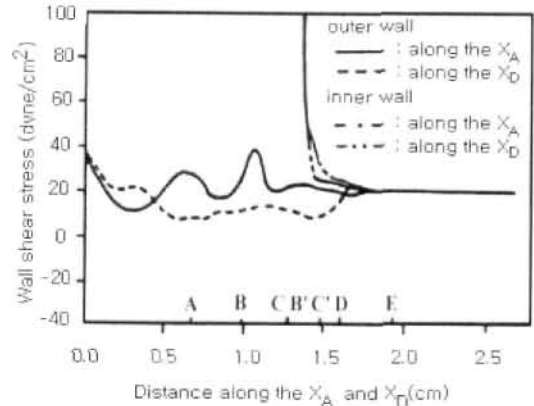
4.3 Review of wall shear stress dependent hypothesis

The development of atherosclerosis strongly suggests the importance of fluid mechanics in atherosclerosis. The flow patterns in the complex geometrical sites such as the carotid and coronary arteries exhibit non-uniform wall shear stress. Two types of shear stress regions are of interest : high shear stress and low shear stress.

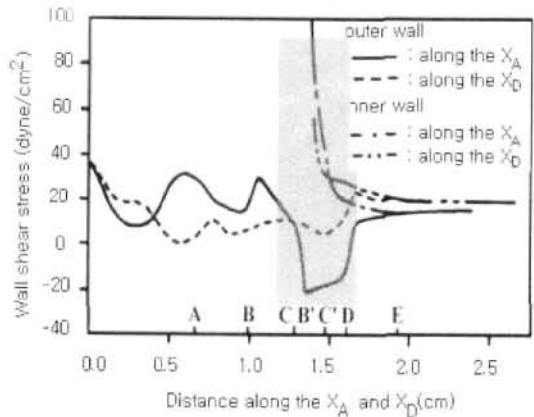
The distributions of wall shear stress in the pulsatile flow were different between the acceleration and deceleration phases as shown in Fig. 9. The highest value of the inner wall shear stress and the lowest value of the outer wall in the LAD artery were more prominent in the deceleration phase. It was noted that the wall shear stress of the outer wall varied, initially. Then, it decreased approaching bifurcation, and represented its lowest value at the bifurcation site, prominent in the deceleration phase of the outer wall of the LAD artery. In acceleration phase, there were no definitive abrupt changes in the outer wall, from inlet to both branching arteries.

The high shear stress region was that at a flow divider of the bifurcation. At the dividers of bifurcations and branches the shear stress became much greater than 100 dyne/cm^2 . The intima in high shear stress regions was exposed to higher shear stress. Thus, the endothelial cells at the flow divider were damaged.

As discussed in the previous section the recirculating flows resulted in low shear stress regions. Mechanical injury was also caused by low shear stress. Low-shear areas included the wall opposite to a branch, the proximal wall of a branch vessel, and the inner of the curved area. The effect of these flows on the endothelial cells was fatigue injury, which resulted in endothelial dy-



(a) Acceleration phase



(b) Deceleration phase

Fig. 9 Distributions of wall shear stresses on the inner and outer walls in the coronary artery

function. Specifically, the oscillating wall shear stress causes a series of biological events leading to atherosclerotic lesions and well developed plaque.

The recirculation zone is observed in the sinus of the ICA, and this zone varies during the systole/diastole phase. The wall shear stress varies from the negative value to the positive value during a cycle. It is speculated that the abrupt change of wall shear stress in the sinus may be responsible for the initial formation of atherosclerosis.

5. Summary

In this study, computer simulations and in vivo experiments were conducted to investigate the

generation of atherosclerosis in the carotid and coronary arteries. The abrupt changes of the flow velocity and flow reversal (formation of recirculation) showed in the outer curved region of the left coronary artery around the bifurcation area. In approaching the bifurcation site, the wall shear stress in the outer wall of the left coronary artery decreased due to the directional change of flow, and finally it showed its lowest value at the branching site of the outer wall. The wall shear stress at both branching apexes was highest in the inner wall, and then it decreased gradually. However, the highest value of the inner wall and the lowest value of the outer wall in the LAD artery were more prominent in the deceleration phase than in the steady flow. This study suggests that temporal and/or spatial fluctuations of the shearing force and flow velocity variation in the same coronary arterial tree may have some interplay with biomechanical and humoral stimuli in the atherogenesis and progression of atherosclerosis. The lesion-prone areas, arterial bifurcations and curvatures usually have temporal and/or spatial fluctuations of the shearing force and flow velocity variation in the same in vivo system.

In this study, it was noted that the velocity profiles were skewed toward the inner wall, showing higher velocity along the inner wall region, while spatial fluctuation and variation of flow velocity between the axial flow and the outer wall of a stagnant flow region were noted distinctively at the curved area of the left coronary artery and on the outer wall of the proximal part of the anterior descending artery around the branching site. In approaching the bifurcation site, the wall shear stress in the outer wall of the left coronary artery decreased due to the directional change of flow, and eventually showed its lowest value at the branching site of the outer wall. Conversely, the wall shear stress of the inner wall was highest in the branching apex. Under the physiologic condition, it was reported that the recirculation zone formed by the abrupt change of blood flow might have an important role in early atherosclerosis and that the turbulent transformation of flow occurred more readily in the deceleration phase of pulsatile flow. We also showed that the flow

reversal and the recirculation region were more prominent in the deceleration phase of pulsatile flow and that the portion of low wall shear stress occurred at the same site as the recirculation area shown in the result taken from velocity calculation.

Finally, these results can be used to understand the pathogenesis of atherosclerosis, and to predict its progression or restenosis in coronary intervention. Moreover, it is expected that these efforts can be used in coronary interventions with site-specific delivery of the genetic therapy on intimal proliferation to prevent restenosis of coronary arterial disease, and it can be applied to vascular surgical designs in coronary artery bypass graft. The emerging paradigm of biomechanical activation of endothelial cells promises to be a conceptually rich and pathophysiologically relevant area for future investigation. However, there existed some limitations in practically applying these results to clinical settings. And there are marked individual variations in vascular structure and hemodynamics. It will be necessary that further experiments be undertaken under various conditions including in vitro and in vivo biologic study. This will be reported in our next study on the role of hemodynamics in advanced stages of atherosclerosis and conditions after interventions such as coronary artery bypass grafting and percutaneous angioplasty.

Acknowledgments

This work was supported by grant No R01-2002-000-00561-0 from the Basic Research Program of the Korea Science & Engineering Foundation.

References

- Caro, C G, Fitz-Gerald, J M and Schroter, R C, 1971, "Atheroma and Arterial Wall Shear Observation, Correlation and Proposal of a Shear Dependent Mass Transfer Mechanism for Atherogenesis," *Proc R. Soc. B*, Vol 177, pp 109~159.
- Cho, M T, Roh, H W, Suh, S H and Kim,

J S, 2002, "Pulsatile Flow Analysis of Newtonian Fluid in Circular Tube," *KSME (B)*, Vol 26, No 1, pp 1585~1596

Fox, J A and Hugh, A E, 1966, "Localization of Atheroma a Theory Based on Boundary Layer Separation," *Br Heart J*, Vol 28, No 3, pp 388~399

Fry, D L, 1972, "Response of the Arterial Wall to Certain Physical Factors Atherogenesis Initiating Factors," A Ciba Foundation Symp, ASP, Amsterdam, The Netherlands, pp 40~83

Lee, B K, Kwon, H M, Hong, B K, Park, B E, Suh, S H, Cho, M T, Lee, C S, Kim, M C, Kim, C J, Yoo, S S and Kim, H S, 2001, "Hemodynamic Effects on Atherosclerosis-Prone Coronary Artery wall Shear Stress/Rate Distribution and Impedance Phase Angle in Coronary and Aortic Circulation," *Yonsei Med J*, Vol 42, No 4, pp 375~383

Suh, S H, Roh, H W and Kim, J S, 2003, "Effect of the Velocity Waveform of the Physiological Flow on Hemodynamics in the Bifurcated Tube," *KSME International Journal*, Vol 17, No 2, pp 296~309

Suh, S H, Roh, H W, Yoo, S S and Kwon, H M, 1996, "Numerical Simulation of Blood Flow in the Human Left Coronary Artery," *The 9th Int Symp on Trans Phenomena in the Thermal-Fluids Eng*, pp 91~96

Texon, M, Imparato, A M and Helpert, M., 1965, "Role of Vascular Dynamics in the Development of Atherosclerosis," *JAMA*, Vol 194, pp 168~172

Tucker, C and Mylon, I C, 2001, "NF- κ B Pivotal Mediator or Innocent Bystander in Atherogenesis?" *J Clin Invest*, Vol 107, No 3, pp 255~264